

# Total quenching of $F$ -center luminescence and photoionization by $\text{OH}^-$ molecular defects in KCl

Laercio Gomes\* and Fritz Luty

Physics Department, University of Utah, Salt Lake City, Utah 84112

(Received 3 April 1984)

The well-established electronic processes originating in the relaxed excited  $F$ -center state of KCl, KBr, . . . , become drastically changed by the presence of high (mole fractions of  $10^{-3}$ – $10^{-2}$ ) concentrations of  $\text{OH}^-$  defects. Both the  $F$ -center luminescence and the photoionization (as measured by photoconductivity or  $F \rightarrow F'$  conversion) decrease systematically with  $\text{OH}^-$  doping. In quenched crystals with statistical defect distribution, the observed behavior can be fitted to a model involving total luminescence and photoionization quenching for a critical distance  $R_c \leq 5$  lattice parameters between  $F$ -center and  $\text{OH}^-$  defect. Light-induced migration of the  $F$  centers leads to total association of all  $F$  centers and  $\text{OH}^-$  defects, decreasing further the small remaining  $F$ -center luminescence and photoconductivity. The end point of this aggregation is an  $F\text{-OH}^-$  pair [ $F_H(\text{OH}^-)$ ] center, characterized by a strong broadening and red shift of the  $F$  band. Measurements of the time-dependent  $F$  ground-state repopulation under high-power pulsed-laser excitation show that the  $\text{OH}^-$ -perturbed  $F$  centers have nonradiative decay rates shorter than  $\sim 10$  nsec. Various physical mechanisms for the unexpected and dramatic changes in  $F$ -center deexcitation are discussed, leading to the plan of a set of critical and clarifying new optical experiments.

## I. INTRODUCTION

The richness of modern color-center physics and applications is, to a large extent, based on the fact that the simple  $F$ -center defect can be used as an "elementary building block" for the construction of a large variety of  $F$ -aggregate centers. Controlled production of these aggregates is achieved by optical ionization of  $F$  centers above  $\sim 230$  K, which leads to thermally activated diffusion of the anion vacancy.<sup>1</sup> Any type of defect in the crystal may act as a trapping site for the migrating vacancy, such that after recapture of the ionized electron an  $F$ -aggregate center is formed. Four types of primary  $F$ -aggregate centers are known: The association of an  $F$  center with another  $F$  center yields the  $\langle 110 \rangle$ -oriented  $F_2$  center, the association of an  $F$  center with a cation impurity (such as  $\text{Li}^+$  or  $\text{Na}^+$  in KCl) yields the  $\langle 100 \rangle$ -oriented  $F_A$  center, the association of an  $F$  center with a divalent-cation-cation-vacancy pair yields the center  $F_Z$ , and the association of an  $F$  center with an anionic defect yields the  $\langle 110 \rangle$ -oriented  $F_H$  center. For the first three types of  $F$  center, the reduction in symmetry by the defect association produces pronounced absorption and emission changes compared to the  $F$  center, as well as optical anisotropic properties. From these primary aggregates a sequence of more complex secondary aggregates, involving more  $F$  centers or defect partners, can be formed in most cases. The richness of optical and photochemical behavior is further increased by the fact that most aggregate centers exist in lattice-neutral as well as in electron-excess or electron-deficient form (such as  $F_2$ ,  $F_2^-$ , and  $F_2^+$ ).

In the alkali halides with NaCl structure, only one single type of  $F_H$  center has so far been realized and investigated, namely the association of an  $F$  center with an  $\text{H}^-$  defect on  $\langle 110 \rangle$  neighboring sites.<sup>2,3</sup> The perturbation

caused by exchanging one of the 12 next-nearest halide neighbors by an  $\text{H}^-$  ion is extremely weak, so that the normal  $F$ -center absorption, emission, and radiative lifetime are only very slightly modified. In fact, the existence of the  $F_H(\text{H}^-)$  configuration could only be verified observing the high-energy  $\text{H}^-$  local mode—split into three components by the reduced symmetry—in the resonance Raman spectrum of the slightly perturbed  $F$  center.

In a program directed both toward interesting scientific and application aspects, we have raised the question of whether  $F$  centers can be associated with diatomic molecular defects ( $\text{XY}^-$ ), thus forming  $F_H(\text{XY}^-)$  centers. As molecular defects have rotational degrees of freedom, can be aligned by electric fields or stress, and possess high-frequency internal stretching modes, interesting and novel interaction effects with neighboring  $F$  centers can be expected. This expectation was richly rewarded in the first realization of this type, an  $F_H(\text{CN}^-)$  center, which we reported recently.<sup>4</sup> The association of an  $F$  center to a  $\text{CN}^-$  defect produces—similar to the above-mentioned  $F_H(\text{H}^-)$  case—a small red shift of both the normal  $F$  absorption and emission. Beyond this (rather unexciting) small perturbation, however, a novel and highly interesting interaction effect appears: Pumping of the optical cycle of the perturbed  $F$  center leads to the excitation of the  $\text{CN}^-$  internal stretching mode, and, consequently, to the emission of vibrational fluorescence (at  $4.8 \mu\text{m}$ ) from the  $\text{CN}^-$  stretching oscillators. As the efficiency for the conversion into vibrational fluorescence is only  $\sim 4\%$ , the reduction in the electronic  $F_H(\text{CN}^-)$  emission strength is hardly noticeable.

In this work we address the above question for similar types or interaction and association effects between  $F$  centers and substitutional  $\text{OH}^-$  defects, starting with the most widely studied hosts, KCl and KBr. The  $\langle 100 \rangle$ -orientational states, and paraelectric<sup>5</sup> and paraelastic<sup>6</sup>

properties, as well as the stretching<sup>7</sup> and librational<sup>8</sup> excitations of  $\text{OH}^-$  defects in these hosts, are well investigated and understood. Among all possible molecular defects,  $\text{OH}^-$  possesses the highest-energy stretching mode,  $\nu_s$ , with  $h\nu_s \approx 0.45$  eV being about one-half of the *F*-center emission energy. Interesting dynamic interaction effects between *F* and  $\text{OH}^-$  centers can be expected and are indeed observed. As we will show in this work, the presence of  $\text{OH}^-$  defects drastically changes (very much *in contrast to*  $\text{CN}^-$  molecules) all the radiative and nonradiative properties of the relaxed excited *F*-center state.

## II. EXPERIMENTAL TECHNIQUES AND APPARATUS

The single crystals of different  $\text{OH}^-$  and  $\text{OD}^-$  dopings were grown in the Utah Crystal Growth Laboratory. The actual  $\text{OH}^-$  and  $\text{OD}^-$  content in the samples was determined by ir or uv measurements of the vibrational or electronic  $\text{OH}^-$  absorption, using the quantitative calibrations from Ref. 9. Absorption measurements were performed in a Cary-Varian model 17 DX spectrometer. Emission measurements were performed using a 514-nm Ar-ion laser for excitation, and a cooled PbS detector with appropriate filter or a grating monochromator for detection. Excitation spectra of the emission were taken with a 1000-W xenon lamp in connection with a tunable grating monochromator. Photoconductivity measurements were done on  $\sim 1$ -mm-thick samples, under an applied dc field of 2000 V/cm, illuminated with monochromatic *F* light through fine-metal-net electrodes pressed to the sample, and with the use of a Keithley model 610-A electrometer for current measurements. In the absorption-modulation experiments, 514-nm light from an Ar<sup>+</sup>-ion laser was used for monitoring the *F*-band transmission. Periodically repeated pulses ( $\sim 3$  MW, and of  $\sim 10$  nsec duration) from an excimer-laser-pumped dye-laser system were used for the pulsed depopulation of the *F*-center ground state. The effect of this pulse excitation on the probe beam was monitored in its time dependence with a Si detector (response time of  $\sim 3$  nsec), and displayed and recorded on an oscilloscope.

## III. EXPERIMENTAL RESULTS

In this work we performed parallel experiments with various techniques on two types of defect systems, which we introduce with the experiments summarized in Figs. 1 and 2. The first type of system consists of additively colored  $\text{OH}^-$  (or  $\text{OD}^-$ ) doped crystals which have been freshly quenched from high temperature and immediately cooled without light exposure to low temperatures. Figure 1(a) shows the low-temperature (10-K) *absorption spectra* of two samples with different high  $\text{OH}^-$  doping levels, in comparison to a pure  $\text{OH}^-$ -free sample. As can be seen, the *F* absorption is nearly indistinguishable in the three samples, identical in peak position, and with only a very small ( $\sim 3\%$ ) broadening effect from the presence of the  $\text{OH}^-$  defects showing up. This evident insensitivity of the *F* absorption to the  $\text{OH}^-$  defects is in pronounced contrast to the strong effect on the *F* emission caused by the  $\text{OH}^-$  defects [Fig. 1(b)]: Without changing the spec-

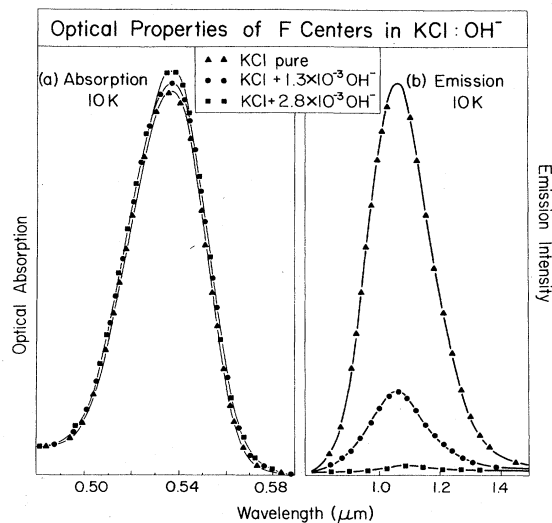


FIG. 1. (a) *F*-center optical absorption and (b) emission at 10 K in additively colored, quenched KCl crystals—pure and with two high  $\text{OH}^-$  dopings.

tral shape or position of the *F* emission, its strength becomes drastically decreased by increasing amounts of  $\text{OH}^-$  defects. Evidently, even in this “quenched,” i.e., statistically distributed defect, case, the presence of nonassociated  $\text{OH}^-$  defects produces strong *F*-center luminescence quenching.

The second type of system used in our experiments consists of the same colored  $\text{OH}^-$ -doped crystals, which, however, after quenching (and initial low-temperature measurements) were illuminated with rather small doses of visible light at  $-30^\circ\text{C}$ . Figures 2(b) and (c) show the effect of increasing light exposure on crystals of two different  $\text{OH}^-$  dopings: The original normal *F* absorption becomes increasingly broadened and red-shifted by this process. For comparison, in Fig. 2(a) we show that the same quantity of light exposure in a pure KCl crystal produces a negligibly small effect on the *F* absorption. Only after considerably longer light exposure at higher tem-

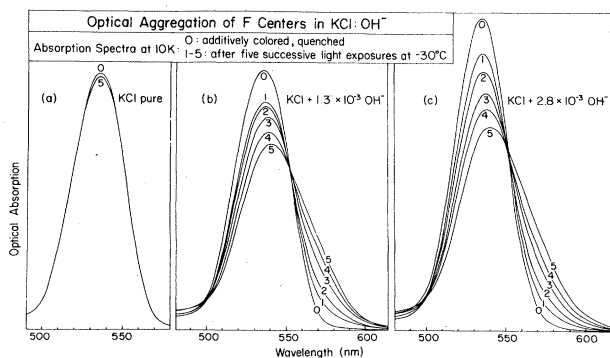


FIG. 2. Visible absorption spectra at 10 K of additively colored KCl, quenched and after five successive *F* light exposures of  $-30^\circ\text{C}$ , for (a) pure KCl and with (b) and (c) two high  $\text{OH}^-$  dopings.

peratures will the normal intrinsic  $F$ -aggregate-center,  $F_2, F_3, \dots$ , absorption develop in this pure crystal. This clearly demonstrates that the employed light exposure at  $-30^\circ\text{C}$  was completely insufficient to achieve thermal diffusion of photoionized  $F$  centers over a sufficiently wide range to form  $F$ -center pairs. The same treatment applied to the  $\text{OH}^-$ -doped crystals, however, leads to strong changes in the  $F$  absorption. The evident conclusion from these results is the following: In the crystals with  $\text{OH}^-$  doping (about 2 orders of magnitude higher than the  $F$  concentration), very few diffusion jumps of the photoionized  $F$  centers can lead to association with one of the abundantly present  $\text{OH}^-$  defects. The resulting broadened and red-shifted absorption spectra in Figs. 2(b) and (c) are characteristic of mixtures of  $F$  centers with increasing numbers of closely associated  $F$  and  $\text{OH}^-$  centers, i.e.,  $F_H(\text{OH}^-)$  centers.

The described process of  $F$ -center- $\text{OH}^-$  association can be reversed, leading to thermal dissociation of the  $F_H(\text{OH}^-)$  complex. Under annealing of a fully aggregated  $F_H(\text{OH}^-)$ -center system in the dark close to or higher than room temperature, one observes a gradual change of the broadened  $F_H(\text{OH}^-)$  absorption back into the original  $F$ -center absorption. By monitoring this backconversion of the optical absorption [curve 5 $\rightarrow$ 0 in Figs. 2(b) and (c)] after annealing for various time periods at different temperatures, we found that the thermal dissociation process can be described by a single Arrhenius relation. The results of these measurements (Fig. 3) yield an activation energy of 0.94 eV and an attempt frequency of  $10^{12} \text{ sec}^{-1}$ . Comparison in Fig. 3 to corresponding measurements of the thermal dissociation of  $F_A(\text{Li})$  centers<sup>10</sup> gives very close coincidence, showing that both defect complexes have very similar thermal stability. In both cases, the  $F$  center leaves the site of association to the defect ( $\text{Li}^-$  or  $\text{OH}^-$ , respectively) in a step-diffusion process, requiring an activation energy of  $\sim 1$  eV. For practical purposes, it is important that the  $F_H(\text{OH}^-)$  center has a mean lifetime

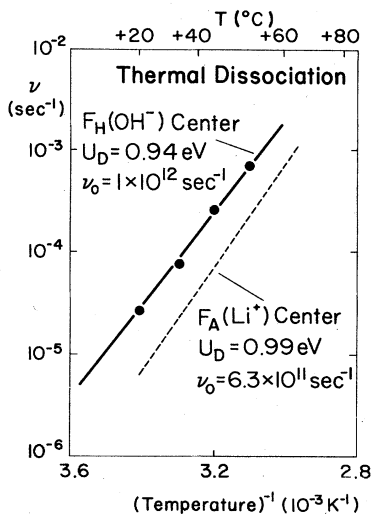


FIG. 3. Arrhenius plot of the thermal dissociation rate  $\nu_D$  of  $F_H(\text{OH}^-)$  centers in KCl [in comparison to  $\nu_D$  of  $F_A(\text{Li}^+)$  centers].

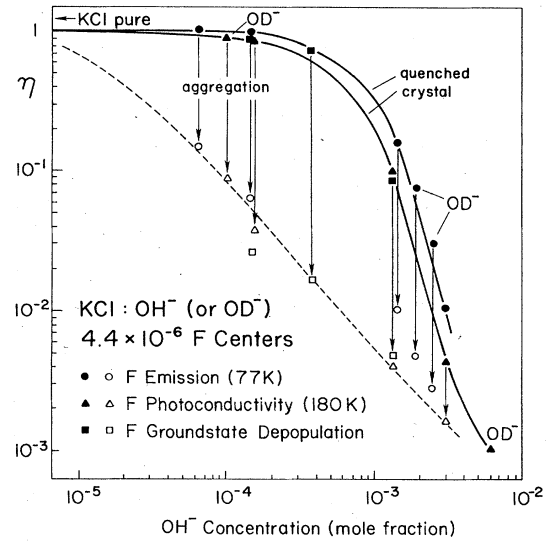


FIG. 4. Double-logarithmic plot of  $F$ -center emission, photoconductivity, and ground-state depopulation as a function of  $\text{OH}^-$  concentration, for the quenched and optically aggregated KCl crystals.

of  $\sim 10$  h at room temperature (RT), so that optically aggregated crystals can be handled and transferred at RT in this time span.

All experiments in this work were performed first on quenched (statistically distributed) systems and subsequently on the same samples after the above-described  $F \rightarrow \text{OH}^-$ -defect association procedure. Figure 4 summarizes the results of various experiments on both quenched and optically aggregated crystals as a function of  $\text{OH}^-$  doping. The first result is the pronounced effect on the quantum efficiency of the  $F$  emission  $\eta_{\text{lum}}$  already introduced for quenched crystals in Fig. 1. While  $\text{OH}^-$  concentrations up to  $\sim 10^{-4}$  mole parts have essentially no effect, a drastic decrease of  $\eta_{\text{lum}}$ —by approximately 2 orders of magnitude—takes place when increasing the  $\text{OH}^-$  concentration toward  $10^{-2}$  mole parts. Subsequent optical aggregation of the  $F$  centers (as described in Fig. 2) produces a further decrease of the  $F$  emission, as indicated by arrows in Fig. 4. Even in crystals with small  $\text{OH}^-$  content ( $N < 10^{-4}$ ), which in the quenched state showed full efficiency,  $\eta_{\text{lum}}$ , the  $F \rightarrow \text{OH}^-$  optical aggregation process produces sizable  $F$ -emission reduction. For the crystals with highest  $\text{OH}^-$  doping, on the other hand, which in the quenched state displayed already strongly reduced emission, the further reduction by optical aggregation is relatively small.

While for unperturbed dilute  $F$  centers at low temperatures the radiative deexcitation process is the only fundamental transition from the relaxed excited state (RES), toward higher temperature ionization of the electron into the conduction band becomes increasingly effective with an Arrhenius-type rate behavior.<sup>11</sup> This ionization process can be monitored with high sensitivity by photoconductivity measurements.<sup>12</sup> Figure 5 displays (in logarithmic scale), in the upper curve, a typical  $F$  photoconduc-

tivity temperature dependence for a pure KCl crystal. The strong increase over more than 2 orders of magnitude with temperature reflects the Arrhenius-type ionization process from the RES, bringing it to full quantum efficiency and saturation at higher temperatures.

The two lower solid curves in Fig. 5 show identical photocurrent measurements for two crystals with high  $\text{OH}^-$  concentrations. Over the entire temperature range the photoconductivity is found to be reduced by approximately 1 and 1–2 orders of magnitude, respectively, for the two  $\text{OH}^-$ -doped crystals. Subsequent optical aggregation of the  $F$  centers to the  $\text{OH}^-$  defects produces a further reduction (indicated by arrows) to the dotted curves. Again, as in the luminescence case, this further reduction is much stronger for lower as compared to higher  $\text{OH}^-$  concentrations. From raw data of this type, we plot the relative reduction of the photocurrent at 180 K into the same, preceding diagram (Fig. 4, triangles) used for the luminescence reduction. As can be seen, the  $F$  luminescence and photocurrent dependence on the  $\text{OH}^-$  content match extremely well, both for the quenched and optically aggregated case.

The electrons thermally released from the RES and producing the photocurrent are known to become trapped eventually in other  $F$  centers, forming the  $F'$  defect. The rate of photochemical  $F \rightarrow F'$  conversion parallels the photocurrent and can be used as an alternative method of determining the photoionization rate.<sup>11</sup> We have not made quantitative measurements of the  $F \rightarrow F'$  conversion rate, but have only determined the equilibrium  $[F']/[F]$  value achievable at 150 K under constant  $F$  light irradiation. Figure 6 shows the result for crystals of various  $\text{OH}^-$  dopings in both the quenched and optically aggregated state. The  $\sim 55\%$  reduction  $\Delta F_{\text{abs}}$  of the  $F$  band due to  $F \rightarrow F'$  conversion achievable in pure crystals is drastically reduced for  $\text{OH}^-$  concentrations above  $10^{-4}$  in

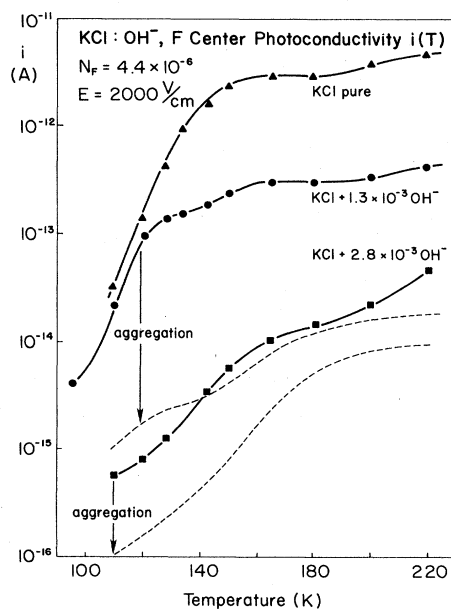


FIG. 5. Temperature dependence of  $F$ -center photoconductivity for pure KCl and with two high  $\text{OH}^-$  dopings.

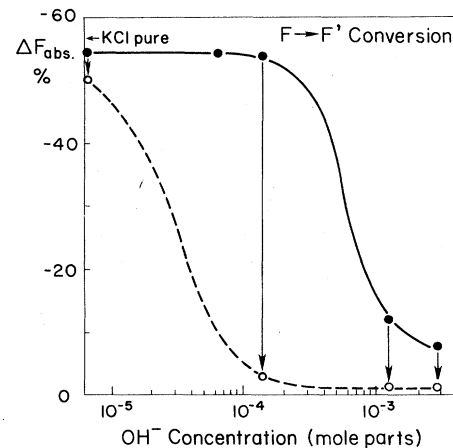


FIG. 6. Maximum reduction  $\Delta F_{\text{abs}}$  of  $F$  band due to  $F \rightarrow F'$  conversion as a function of  $\text{OH}^-$  doping, for quenched and optically aggregated crystals.

quenched crystals. After optical aggregation this reduction occurs already at much lower  $\text{OH}^-$  doping. The  $[F']/[F]$  ratio is a dynamical equilibrium of  $F \rightarrow F'$  production and optical  $F'$  destruction. These results confirm the photoconductivity results: Both show that the presence of  $\text{OH}^-$  defects in the crystal, either statistically distributed or preferentially associated to  $F$  centers, reduces the ionization process from the relaxed excited  $F$  state.

In a third type of experiment (very important for the interpretation), we measure the time dependence of the  $F$  absorption strength after high-power pulse excitation in the  $F$  band. Figure 7 displays a duplicate of original oscilloscope traces, monitoring, using 514-nm  $\text{Ar}^+$ -ion laser light, the optical transmission of the  $F$  band as a function of time. Application of the ( $\sim 10$ -nsec) pump laser pulse depopulates the  $F$ -center ground state, causing a strong increase in the intensity of the probe beam, which is reversed by the gradual return of the electrons from the excited to the ground state. The measured lifetime of this

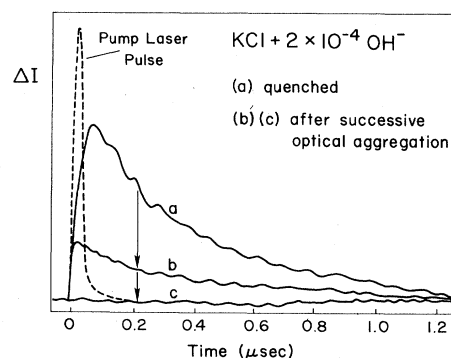


FIG. 7. Original measurement examples of the time-dependent  $F$ -center transmission after pulsed-laser excitation for low- $\text{OH}^-$ -doped crystal, (a) quenched and (b) and (c) after two successive optical aggregations. The dotted line gives a measurement of the exciting-laser pulse with the same detector.

“ground-state–repopulation” process ( $\tau \approx 0.6 \mu\text{sec}$ ) in this very-low- $\text{OH}^-$ -doped KCl, is the same as the radiative lifetime of the normal  $F$  emission, as expected. Two successive optical aggregations of the quenched sample reduce, however drastically, the observed transmission increase without changing its time constant. In Fig. 8 we display averaged results from similar measurements under variation of both  $\text{OH}^-$  content and optical aggregation procedure. The pure crystal in quenched form shows the largest initial transmission increase, with  $\sim 81\%$  of the  $F$  center being depopulated at  $t=0$ . With increasing  $\text{OH}^-$  concentration the size of the transmission change is drastically reduced, keeping the same time constant. Optical aggregation affects the pure  $F$ -center case only very slightly, while producing very sizeable reductions of the transient transmission change for the  $\text{OH}^-$ -doped crystals. Plotting the size of the relative transmission increase as a function of  $\text{OH}^-$  content (for both the quenched and optically aggregated crystal) into our comprehensive diagram (Fig. 4) yields a nearly perfect match to the data on  $F$  luminescence and photoconductivity.

In a final measurement we compare KCl: $\text{OH}^-$  with  $F$  centers in two stages [Fig. 9(a)]: (I) in the quenched state, i.e., containing mostly unassociated  $F$  centers, and (II) after heavier optical aggregation at  $-10^\circ\text{C}$ , which produces not only  $F_H(\text{OH}^-)$  centers (as in Fig. 2), but also a small number of  $F_2$  centers, as seen by the weak  $M$  band at 800 nm. In Fig. 9(b) we measure, for these two stages, the total  $F$ - and  $F_2$ -center emission in the (1.0–1.2)- $\mu\text{m}$  regime (broad-band filter) as a function of the monochromatic exciting light tuned between 400 and 800 nm. In the quenched state, stage (I), we observe a peak around 520 nm from the excitation of  $F$  centers (flattened, as expected, at the top due to the high optical density in the  $F$ -band peak). Despite the fact that only a very small

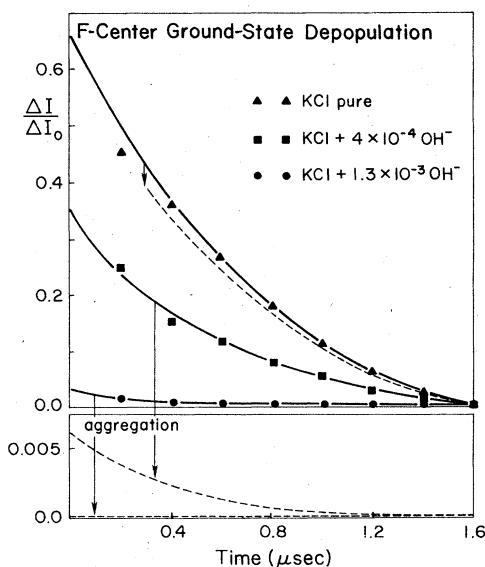


FIG. 8. Averaged results from various time-dependent  $F$ -center measurements after pulsed-laser excitation for pure and  $\text{OH}^-$ -doped crystals, quenched and after optical aggregation.

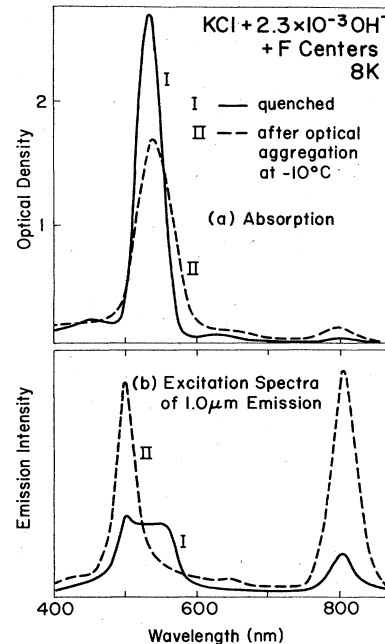


FIG. 9. (a) Optical-absorption spectra and (b) excitation spectra of 1.0- $\mu\text{m}$  luminescence, measured at 8 K in an additively colored KCl: $\text{OH}^-$  crystal before (I) and after (II) optical aggregation at  $-10^\circ\text{C}$ .

number of  $F_2$  centers ( $[F_2] \ll [F]$ ) are present, the  $F_2$  luminescence (seen either under excitation at 800 nm or in the higher-energy transition at 500 nm) is comparable in strength to the  $F$  luminescence. Optical aggregation at  $-10^\circ\text{C}$  [stage (II)] completely eliminates the small initial  $F$  luminescence (as shown earlier in Fig. 4), leading instead to an increase of the  $F_2$ -center luminescence. Evidently, the strong quenching effect of  $\text{OH}^-$  defects, which drastically reduces the  $F$  emission in statistical distribution and totally eliminates it under  $F \rightarrow \text{OH}^-$  aggregation, is not effective at all for the emission of  $F_2$  centers.

Doping of crystals with  $\text{OH}^-$  defects leads inadvertently to the incorporation of  $\text{CO}_3^{2-}$  impurities into the crystal. In order to ensure that the latter impurities were not causing our observed effects, we intentionally doped a crystal with large amounts of  $\text{CO}_3^{2-}$  but small amounts of  $\text{OH}^-$  defects.  $F$ -center luminescence measurements in the crystal definitely showed that the quenching effect was *not* caused by the  $\text{CO}_3^{2-}$ .

#### IV. DISCUSSION

It is evident from the measurements presented in Sec. III that, even in the case of statistically distributed, i.e., essentially nonassociated,  $F$  centers and  $\text{OH}^-$  molecules, a strong interaction effect exists between the two types of defects. This interaction does *not* affect the absorption of the  $F$  center, which is found to be virtually unchanged in its three lowest moments: oscillator strength, energy position, and width [Fig. 1(a)]. It affects, however, in a profound way, the electronic processes occurring after the ab-

sorption in the excited state of the  $F$  center.

Before attempting any explanation of the physical nature of this interaction, we estimate the spatial distance over which this interaction is effective. For the quenched case we assume that both defect species are statistically distributed, and that due to the small  $F$ -center concentration,  $n_F \ll n_{\text{OH}^-}$ , interaction effects between  $F$  centers can be neglected. The fraction of  $F$  centers,  $n(R)/n_F$ , which will have an  $\text{OH}^-$  defect as the closest neighbor between distance  $R$  and  $R + dR$ , is given by

$$\frac{n(R)}{n_F} = \frac{4\pi R^2}{R_0^3} \frac{n_{\text{OH}^-}}{N} \left[ 1 - \frac{n_{\text{OH}^-}}{N} \right]^{(4\pi R^3/3R_0^3)-2} dR, \quad (1)$$

with  $R_0^3 = a^3/4 = 1/N$  ( $a$  denotes the lattice parameter). Integrating Eq. (1) between  $R_1$  and  $R_2$  yields

$$\frac{n(R)}{n_F} \Bigg|_{R=R_1}^{R=R_2} = C \frac{n_{\text{OH}^-}}{N} \frac{1}{\ln(1 - n_{\text{OH}^-}/N)} \times \left[ \left[ 1 - \frac{n_{\text{OH}^-}}{N} \right]^{(4\pi R^3/3R_0^3)-2} \right]_{R=R_1}^{R=R_2}. \quad (2)$$

The normalization constant  $C$  is obtained by assuming that integration from the nearest possible defect distance  $R_1 = 0.7a$  to  $R_2 = 12a$  yields 1 in the above equation, which is quite well justified for the above concentration. Figure 10 shows, in the shaded histogram, the probability of the occurrence of  $F$  centers having the nearest  $\text{OH}^-$  neighbor at a distance  $R$ , calculated from Eq. (2). Obviously, this probability histogram shifts, with increasing  $\text{OH}^-$  concentration, to smaller distances  $R$ .

We can now consider various functional forms for the interaction effect between  $F$  center and  $\text{OH}^-$  defect, responsible for the observed quenching of the  $F$  lumines-

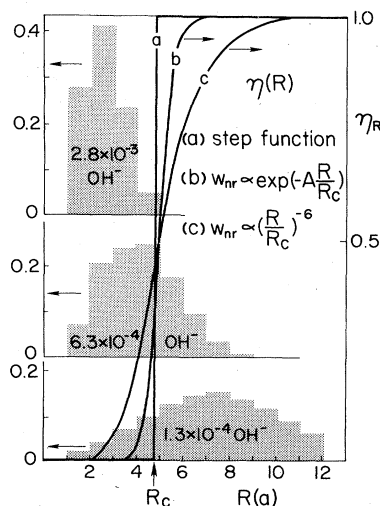


FIG. 10. Shaded areas: Statistical probability (left-hand scale) for the occurrence of  $\text{OH}^-$  defects at a distance  $R$  from  $F$  centers, calculated for three  $\text{OH}^-$  concentrations. Solid lines: Dependence of the efficiency ( $\eta_{\text{lum}}$  or  $\eta_{\text{ion}}$ ) of the excited  $F$  center on the distance  $R$  of the nearest  $\text{OH}^-$  neighbor (right-hand scale), calculated for three assumed  $\eta(R)$  relations.

cence and photoionization. The most simple "step model" assumes that, for distances  $R$  beyond a certain critical value ( $R > R_c$ ), the  $\text{OH}^-$  defect has no effect on the  $F$ -center properties (so that  $\eta_{\text{rad}}$  and  $\eta_{\text{ion}}$  are the normal  $F$ -center values), while, for  $R < R_c$ , luminescence and ionization are completely quenched, i.e.,  $\eta_{\text{lum}} = \eta_{\text{ion}} = 0$ . For this case we obtain, from Eq. (2), for the efficiency  $\eta$ ,

$$\eta = \sum_{R_c}^{\infty} \frac{n_R}{n_F} \times 1 \approx \sum_{R_c}^{12a} \frac{n_R}{n_F} = \exp \left[ -\frac{4\pi}{3} R_c^3 n_{\text{OH}^-} \right]. \quad (3)$$

To test this relation we plot the measured efficiencies (from Fig. 4) logarithmically versus the  $\text{OH}^-$  concentration (Fig. 11). We indeed obtain a very good straight-line dependence, yielding, as a fitting parameter, a critical distance of  $R_c = (4.75 \pm 0.15)a$  lattice parameters, i.e., very close to  $R_c = 5a$ . We can plot the obtained  $\eta(R)$  function into the diagram of Fig. 10, clearly illustrating how the  $\eta(R)$  "step function" divides the statistical distribution into  $F$  centers with either  $\eta = 0$  (for  $R < R_c$ ) or  $\eta = 1$  (for  $R > R_c$ ).

Although this simple step-function model works extremely well and yields the correct magnitude for the mean interaction distance  $R_c$ , it should be replaced by a more realistic gradual  $\eta(R)$  dependence. In order to test possible choices, we assume that a nonradiative transition rate  $\tau_{\text{nonrad}}^{-1}$  competes with the normal radiative transition rate  $\tau_{\text{rad}}^{-1} = 1.73 \times 10^6 \text{ sec}^{-1}$  of the excited  $F$  center, producing a fluorescence quantum efficiency of

$$\eta_{\text{rad}} = \frac{\tau_{\text{rad}}^{-1}}{\tau_{\text{rad}}^{-1} + \tau_{\text{nonrad}}^{-1}}. \quad (4)$$

As the nonradiative rate is produced by interaction between the excited  $F$  center and the nearest  $\text{OH}^-$  defect, the rate should strongly depend on their relative distance,

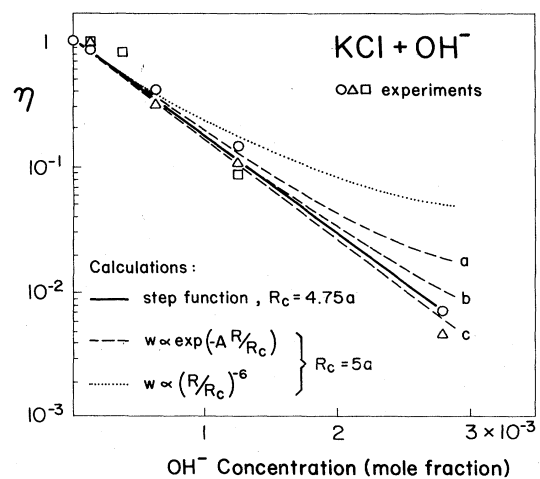


FIG. 11. Logarithmic plot of the measured  $F$ -center emission ( $\circ$ ), photoconductivity ( $\Delta$ ), and ground-state depopulation ( $\square$ ) as a function of  $\text{OH}^-$  concentration. The solid line represents, for  $\eta(R)$ , a simple calculated step function with  $R_c = 4.75a$ ; the dotted curve represents a calculated  $(R/R_c)^{-6}$ ; the dashed curves represent three calculated exponential  $\eta(R)$  dependencies with different  $A$  parameters, as discussed in the text.

$R$ . One possible choice, valid for induced-dipole interaction, is a  $\tau_{\text{nonrad}}^{-1} = AR^{-6}$  dependence. In order to fix the parameter  $A$ , it is reasonable to assume that  $\tau_{\text{nonrad}}^{-1} \cong \tau_{\text{rad}}^{-1}$  (i.e.,  $\eta_{\text{rad}} \cong \frac{1}{2}$ ) at  $R \cong R_c \cong 5a$ . This produces the  $\eta(R)$  dependence shown in curve  $c$  in Fig. 10.

Another possible functional dependence is an exponential one:

$$\tau_{\text{nonrad}}^{-1} = \tau_0^{-1} \exp(-AR). \quad (5)$$

With the (arbitrary) choice of  $\tau_0^{-1} \approx 10^{14} \text{ sec}^{-1}$  [and the condition, as above that  $\tau_{\text{nonrad}}^{-1}(R_c) = \tau_{\text{rad}}^{-1}$ ], we obtain the  $\eta(R)$  dependence, curve  $b$ , in Fig. 10.

In order to translate this into an  $\text{OH}^-$ -concentration dependence, we calculate

$$\eta(n_{\text{OH}^-}) = \sum_{0.7a}^{12a} \frac{n_R}{n_F} \eta(R) \quad (6)$$

for various  $\eta(R)$  choices, and compare the results with the experimental values in Fig. 11. We note the following:

(a) The assumed  $\tau_{\text{nonrad}}^{-1} \propto R^{-6}$  dependence is *not* able to explain the observed behavior.

(b) For an assumed exponential behavior [Eq. (5)], the preexponential factor must be chosen to be rather high ( $\tau_0^{-1} \geq 10^{14} \text{ sec}^{-1}$ ) in order to fit the observed behavior.

In other words, the  $\tau_{\text{nonrad}}^{-1}(R)$  or  $\eta_{\text{rad}}(R)$  dependence must be extremely steep, i.e., close to a step-function dependence (Fig. 10), in order to reproduce the measured concentration dependence. After having established these functional conditions and limits for the distance dependence, we must address the main question of this paper: What is the nature of the  $F$ -center– $\text{OH}^-$  interaction producing the nonradiative  $F$ -center deexcitation?

An attractive interpretation could be the following: The electronic excitation energy of the  $F$  center after relaxation ( $\sim 1 \text{ eV}$ ) is transferred effectively into the excitation of stretching vibrations ( $h\nu = 0.45 \text{ eV}$ ) of a nearby  $\text{OH}^-$  defect. This vibrational excitation of the  $\text{OH}^-$  molecule could then be dissipated either radiatively or nonradiatively.

We have experimentally tested (with techniques similar to those used in Ref. 4) whether an  $\text{OH}^-$  vibrational fluorescence occurs at energies  $< 0.5 \text{ eV}$  under heavy pumping of the  $F$ -center system, both in the aggregated and nonaggregated cases. The result was totally negative: A possible  $\text{OH}^-$  vibrational fluorescence would have to be of very small quantum efficiency,  $\eta < 10^{-3}$ , to be compatible with our negative experiment. Supporting this negative model is the fact that both  $\text{OH}^-$  and  $\text{OD}^-$  produce exactly the same  $F$ -center emission quenching despite the fact that, for  $\text{OD}^-$ , the stretching energy  $\nu(\text{OD}^-)$  is  $\nu(\text{OH}^-)/\sqrt{2} = 0.32 \text{ eV}$ , so that the  $F$ -emission energy is now fitted by  $3\nu(\text{OH}^-)$  instead of  $2\nu(\text{OH}^-)$ .

Another type of interpretation, in principle, could be tried by assuming that the  $F$ -center emission energy is

transferred into librational (rotational) excitation of the  $\text{OH}^-$  ion. The basic energy of the latter<sup>8</sup> is, for KCl  $300 \text{ cm}^{-1}$ , with weaker excitations at higher energies<sup>13</sup> existing at  $383$  and  $407 \text{ cm}^{-1}$ . Here, again, the trouble is that  $\text{OD}^-$ , compared to  $\text{OH}^-$ , has energies which are reduced by about a factor of  $\sqrt{2} = 1.4$ , which makes it highly unlikely that exactly the same excited factor-quenching effect is observed for both types of molecules.

The most important observations, which must be accounted for by a physical model, are the following:

(a) The observed total independence of the  $F^*$  deexcitation efficiency and speed from the large ( $\sim 1.4$ ) isotope variation of both stretching and librational frequencies of the  $\text{OH}^-$ .

(b) The fact that *only* the  $F_{\text{rel}}^*$  center with an extended wave function, but not the excited  $F_2^*$  center with a compact state, becomes luminescence-quenched by distant ( $R \leq 5a$ )  $\text{OH}^-$  defects.

The latter may indicate that the wide spatial extension of the relaxed  $F^*$  center, as measured by electron nuclear double-resonance techniques,<sup>14</sup> causes a rather strong overlap and interaction with the  $\text{OH}^-$  even five lattice parameters away, thus producing delocalized and perturbed excited states. The main question is then, again, why this  $F$ - $\text{OH}^-$  interactive state produces such a short lifetime for nonradiative deexcitation of the electron into the  $F$  ground state.

An attractive explanation for this question is the following: The  $\text{OH}^-$  defect has a large electric dipole, which, in KCl at  $T > 10 \text{ K}$ , reorients extremely rapidly ( $\tau \approx 10^{-10} \text{ sec}$ ). If the positive end of the  $\text{OH}^-$  dipole is directed toward the nearby  $F^*$  center, it works attractively on the  $F$  electron, and could produce an altered spatially and energetically displaced version of the relaxed  $F^*$  state. Reorientation of the  $\text{OH}^-$  dipole, however, turning its negative end toward the  $F$  center, will repel the  $F^*$  electron back to the vacancy into an energy-lowered situation from which it can relax in a radiationless process into the  $F$  ground state. The relevant speed of radiationless deexcitation of the  $F^*$  center would therefore be essentially given by the reorientation rate of the  $\text{OH}^-$  dipole.

Two decisive types of experiments have been started to check, confirm, and explore this explanation:

(1) Measurements with picosecond laser pulses on the radiationless repopulation time of the  $F$  ground state.

(2) Experiments on  $\text{OH}^-$  in host materials with lower dipole-reorientation rates ( $\tau_{\text{dip}}^{-1} < 10^6 \text{ sec}^{-1}$ ) as compared to the  $F$  luminescence rate, at least at low temperatures. If the above explanation is correct, the  $F$  luminescence in the quenched crystal should be only slightly reduced, even with high concentration  $\text{OH}^-$  doping. Under temperature increase, however, the dipole-reorientation rate  $\tau_{\text{dip}}^{-1}$  increases drastically and becomes, at some temperature  $T$ , equal and then higher than  $\tau^{-1}(F_{\text{lum}})$ . For this case one could expect high  $F$  luminescence at low temperature, which, as in KCl, will disappear at higher temperature.

The picosecond-laser-pulse experiments are (1) underway,

in collaboration with El-Sayed *et al.*, and (2) we ourselves are presently involved in performing experiments on host-material variation which show dramatic dependencies of the described phenomena on the molecular reorientation rate. The results of both of these endeavors will hopefully be published soon.

#### ACKNOWLEDGMENTS

This work was supported by the Natural Science Foundation under Grant No. DMR-81-05232. L. Gomes thanks the Brazilian Nuclear Energy Commission (CNEN) for support.

---

\*Permanent address: Instituto de Pesquisas Energeticas e Nucleares (IPEN-CNEN), São Paulo, Brazil.

<sup>1</sup>H. Härtel and F. Lüty, *Z. Phys.* **177**, B69 (1963).

<sup>2</sup>D. S. Pan and F. Lüty, *Phys. Rev. B* **18**, 1868 (1978).

<sup>3</sup>Y. Kondo and F. Lüty, *Solid State Commun.* **40**, 325 (1981).

<sup>4</sup>Y. Yang and F. Lüty, *Phys. Rev. Lett.* **51**, 419 (1983).

<sup>5</sup>S. Kapphan and F. Lüty, *J. Phys. Chem. Solids* **34**, 969 (1973).

<sup>6</sup>H. Härtel and F. Lüty, *Phys. Status Solidi* **12**, 347 (1965).

<sup>7</sup>B. Wedding and M. V. Klein, *Phys. Rev.* **177**, 1274 (1969).

<sup>8</sup>M. V. Klein, B. Wedding, and M. A. Levine, *Phys. Rev.* **180**,

902 (1969).

<sup>9</sup>B. Fritz, F. Lüty, and J. Anger, *Z. Phys.* **174**, 240 (1963).

<sup>10</sup>F. Lüty, in *Physics of Color Centers*, edited by W. B. Fowler (Academic, New York, 1968), Chap. 3.

<sup>11</sup>H. Fedders, H. Hunger, and F. Lüty, *J. Phys. Chem. Solids* **22**, 299 (1961).

<sup>12</sup>G. Glaser, *Ann. Phys. (Leipzig)* **27**, 217 (1936).

<sup>13</sup>David Harrison, Ph.D. thesis, University of Utah, 1970.

<sup>14</sup>L. F. Mollenauer and G. Baldacchini, *Phys. Rev. Lett.* **29**, 465 (1972).